Received: 21 July 2021 | Revised: 19 May 2022 | Accepted: 14 June 2022

DOI: 10.1111/ddi.13596

RESEARCH ARTICLE

Diversity and Distributions WILEY

# Connectivity modelling informs metapopulation structure and conservation priorities for a reef-building species

Carmen L. David[1,2] | Martin P. Marzloff[1] | Antony M. Knights[3] | Phillipe Cugier[1] | Flávia L. D. Nunes[1] | Celine Cordier[1] | Louise B. Firth[3] | Stanislas F. Dubois[1]

[1]IFREMER, DYNECO, Plouzané, France

[2]Marine Animal Ecology, Wageningen University and Research, Wageningen, The Netherlands

[3]School of Biological and Marine Sciences, University of Plymouth, Plymouth, UK

**Correspondence**
Carmen L. David, Marine Animal Ecology, Wageningen University and Research, Wageningen, The Netherlands.
Email: carmen-lucia.david@wur.nl

**Funding information**
Office Français de la Biodiversité; Total Foundation for the Biodiversity and the Sea, Grant/Award Number: 1512 215 588/F

**Editor:** Alana Grech

## Abstract

**Aim:** In coastal marine systems, biogenic reef-building species have great importance for conservation as they provide habitat for a wide range of species, promoting biodiversity, ecosystem functioning and services. Biogenic reef persistence and recovery from perturbations depend on recolonization by new recruits. Characterizing larval dispersal among distant reefs is key to understanding how connectivity shapes metapopulation structure and determines network coherence; all of which are of critical importance for effective conservation.

**Location:** Northeast Atlantic coast and western English Channel, France.

**Methods:** We used a biophysical transport model to simulate larval dispersal of the reef-building polychaete *Sabellaria alveolata*. We combined dispersal modelling and network analysis into a framework aiming to identify key reef areas and critical dispersal pathways, whose presence in the network is vital to its overall coherence. We evaluated changes in dispersal pathways constrained by different connectivity thresholds, i.e., minimum dispersal rate for the presence of a connection. We tested scenarios of sequential loss of reefs: randomly, by habitat quality (a score for reef status and occupancy in an area) or by betweenness centrality metric (*BC*; quantifying the proportion of shortest paths connecting all areas that are passing through any given area).

**Results:** We found that the network of *S. alveolata* reefs forms two main regional clusters, the Atlantic coast and the English Channel, which are connected only through weak sporadic dispersal events. Within each cluster, the network is characterized by relatively high connectivity among neighbouring areas with reefs, maintained even under higher connectivity thresholds. Simulating scenarios of sequential loss of reefs further identified high centrality reefs, those with highest *BC* values, key to network coherence.

**Main conclusions:** Effective conservation of this important reef habitat requires a network of protected areas designed to sustain a combination of locally important source reefs, and those that act as stepping stones connecting distant reefs.

KEYWORDS
betweenness centrality, graph theory, habitat fragmentation, hydrodynamic modelling, larval dispersal, network analysis, resilience

## 1 | INTRODUCTION

Our oceans and coastal seas are fundamentally changing. Increased concentrations of atmospheric greenhouse gases are raising sea surface temperatures and changing ocean circulation patterns (Shin & Alexander, 2020; van Gennip et al., 2017), while the introduction of artificial barriers is further altering pathways to dispersal, contributing to large-scale loss and fragmentation of marine habitats (Bishop et al., 2017; Firth et al., 2016). Increasingly, conservation efforts like Marine Protected Areas (MPAs) are considered necessary to counteract the negative effects of environmental change and anthropogenic activities on marine life (Bunn et al., 2000; Treml et al., 2008). However, our understanding of how habitat loss and fragmentation disrupt the connectivity corridors among MPAs, that are fundamental to the maintenance and persistence of existing biodiversity and marine communities, remains largely unexplored.

In marine systems, the production and dispersal of planktonic early life-history stages is a key determinant of spatial organization of species across local and seascape scales (James et al., 2019). Ensuring connectivity is argued to be one solution to biodiversity loss and a key tenet of sustainable ecological networks (Gonzalez et al., 2017). The dispersive larval stage is particularly important as it contributes to local population persistence through self-recruitment (Cowen & Sponaugle, 2009; Paris et al., 2007; Pineda et al., 2010) and resilience to disturbance via re-colonization (Burgess et al., 2014). Studying this dispersive stage provides a means to understand population connectivity, defined as the exchange of individuals among distinct populations (Cowen & Sponaugle, 2009). This exchange of individuals is fundamental to the structural connectedness of a network of otherwise isolated populations (sensu, a metapopulation), and is considered critical to our understanding of metapopulation structure and dynamics (Cowen et al., 2007; Jones et al., 2007).

Networks of marine populations that are constrained by natural topography, such as coastline configuration, can be more or less linearly connected, imparting higher importance to some sites over others (Kininmonth et al., 2010; Urban & Keitt, 2001; Watson et al., 2011). Understanding connectivity in such networks helps to identify key populations that contribute more than others to overall network functioning and coherence (Bodin & Saura, 2010; Urban et al., 2009), and in the setting of conservation priorities (Hastings & Botsford, 2006). The notion of network coherence in particular refers to the deviation from consensus, or how robust the network structure is in the presence of stochastic disturbances (Patterson & Bamieh, 2014). There are several tools available for estimating marine connectivity, and describe the structure of metapopulation networks. Physical tags such as radio or satellite trackers can be used to directly measure connectivity (Le Bris et al., 2013), but these are not feasible for small organisms such as larvae or plant propagules. Alternatively, indirect measures such as molecular tools can be used to infer gene flow and migration rates (Gaggiotti et al., 2004; Liggins et al., 2013), or coupled biological and hydrodynamic (biophysical) models can be used to predict dispersal of particles (North et al., 2009; van Sebille et al., 2018). Recently, biophysical models have been used extensively to estimate connectivity in fish and benthic invertebrate populations, and test hypotheses related to the effects of pelagic larval duration (Cowen et al., 2007; Treml et al., 2012), dispersal distance (Cowen et al., 2006; Shanks et al., 2003), or larval swimming behaviour (James et al., 2019) on propagule dispersal by ocean currents (Knights et al., 2006; Nicolle et al., 2017).

In coastal marine systems, animal ecosystem engineers like corals, bivalves and polychaetes constitute important biogenic reef habitats for conservation and have long been recognized for the ecosystem services that they provide (Beck et al., 2011; Dubois et al., 2006; Lemasson et al., 2017). The biodiversity associated with biogenic reef habitats is often higher than the surrounding environment and can vary with the evolution and ecological status of these habitats (Dubois et al., 2002; Jones et al., 2018). Despite their important role in ecosystem structure and functioning, biogenic reef habitats are considered among the most threatened globally (Beck et al., 2011; Chaverra et al., 2019) and their effective protection requires an in-depth understanding of their population dynamics, connectivity and ecology (Knights et al., 2014; Piet et al., 2015).

In Europe, the polychaete *Sabellaria alveolata* (L.) is an important intertidal reef-builder along the Atlantic coast of Europe, extending from Ireland to Mauritania (Curd et al., 2020). The French coast supports the largest reefs in Europe; extending >100 ha and >1.5 m height in Mont-Saint-Michel Bay, (Noernberg et al., 2010). *S. alveolata* has a biphasic life cycle with sessile adults, and a planktonic dispersive larval phase (Dubois et al., 2007; Wilson, 1970). While spawning can occur throughout the year, two main peaks are typically observed; in late spring (around May) and late summer (around September) (Curd et al., 2021; Dubois et al., 2007). This species can be locally common but may undergo localized extirpation following natural and anthropogenic perturbations (Dubois et al., 2002, 2006; Firth et al., 2015, 2021b; Plicanti et al., 2016). The reefs are protected under Annex I of the EC Habitats Directive (Council Directive EEC/92/43 on the Conservation of Natural Habitats and of Wild Fauna and Flora).

Despite the importance of conservation and protection afforded to *S. alveolata* by European legislation, the reefs are classed as data-deficient habitats in many regions (e.g., Bertocci et al., 2017; Firth et al., 2021a), and the number of recorded observations of this species remains limited (Curd et al., 2020). The status monitoring is lacking over the entire distribution and there is little known about how discrete reefs might function and persist as a regional entity through connectivity. Given that current alterations in environmental

conditions and anthropogenic stressors pose threats to *S. alveolata* (Firth et al., 2021b; Plicanti et al., 2016), a better understanding of the distribution and, importantly, connectivity of this species is needed. Such information will shed light on metapopulation (i.e., network of interconnected populations) functioning and resilience to disturbance, and will pinpoint areas for conservation prioritization. Here, we used a biophysical transport model to simulate large-scale dispersal of larval *S. alveolata* on the Atlantic coast of France. We synthesized multi-year larval dispersal events into a structural network to: (1) describe connectedness across the reefs network, (2) test the resilience of the network to perturbation, allowing the stability of the regional *S. alveolata* metapopulation and its potential for fragmentation to be assessed, and (3) identify populations of local and regional importance to network structure and coherence. The outcome of integrated dispersal modelling and network analysis will provide a baseline framework for the effective regional management of this important habitat.

## 2 | METHODS

Here, we combined hydrodynamic modelling and graph theory to assess regional connectivity and to identify local zones that were either key to maintaining network coherence or were at high risk of becoming isolated, therefore constituting protection priorities. The general approach was to use a hydrodynamic ocean model with a transport module to simulate dispersal of larval *S. alveolata* on the French Atlantic and Western English Channel (hereafter Atlantic and Channel) coasts (Figure 1a, inset c). This region represents the core of *S. alveolata* distribution and supports the largest known reefs. Moreover, this region encompasses the only reefs that are regularly monitored, therefore providing the necessary baseline information on reef status and occupancy to support a study such as ours. Understanding connectivity among these reefs and their resilience will be of critical importance for extending our understanding of this species, particularly in regions that are data poor. Network analysis was then used to integrate seasonal and annual dispersal events among coastal zones with reefs. We selected two network metrics to characterize the network structure, and two operations to evaluate changes in the network, e.g., the fragmentation potential. We further compared scenarios of reef loss, whose selection criterion could be used as effective conservative strategies.

### 2.1 | The hydrodynamic ocean model

The hydrodynamic conditions on the Atlantic and Channel coasts were simulated using the fully validated ocean model MARS3D (Model for Application at Regional Scale; https://mars3d.ifremer.fr/docs/documentation.html) (Lazure et al., 2009; Lazure & Dumas, 2008) with the configuration MANGA2500. The model domain extends between 41°N and 55°N latitude and 5°E to 16°W longitude. The regular numerical grid has a 2.5 km horizontal resolution and 40 sigma vertical layers. Open boundaries and initial conditions were provided by the larger-scale model Mercator with a resolution of 0.0833°. Hourly atmospheric forcing was provided by the Meteo-France ARPEGE HR model with a 0.1° spatial resolution. River discharge values, including Garonne, Vilaine and Loire rivers, were obtained from time series at daily frequencies provided by the French freshwater office database (http://www.hydro.eaufrance.fr).

Oceanic circulation over the Atlantic shelf is predominantly poleward, and follows the shelf topography with an average speed of 3 $cm\,s^{-1}$ (Le Boyer et al., 2013). Atlantic coastal circulation is driven by tides, dynamic winds and density currents from river outflows (Koutsikopoulos & Le Cann, 1996), while the Channel circulation is dominated by strong tidal currents (Salomon & Breton, 1993). Where the Atlantic and Channel meet, the water circulation forms a biogeographic border between the temperate and cold-temperate provinces (Figure 1a) (Spalding et al., 2007). Here, the Ushant Sea, at the western tip of the French coast, is characterized by strong thermal fronts, particularly during spring–summer, acting as a barrier to dispersal (Kelly-Gerreyn et al., 2006).

In addition to simulating oceanographic conditions along the northeast Atlantic shelf, MARS3D has previously been coupled with a pelagic ecosystem model, ECO-MARS3D, developed and validated against historical data (Ménesguen et al., 2019), and was also used to investigate the dispersal of fish and benthic invertebrate larvae coupled with a Lagrangian (Ayata et al., 2010; Huret et al., 2010) and an Eulerian transport model (Ayata et al., 2009).

### 2.2 | Transport module

We used a Eulerian approach to simulate larval dispersal by tracking concentration of suspended particles. Specifically, we used the transport module of the ocean model MARS3D, which was run online with an adaptative time step of ~135 s. Larval dispersal was calculated by solving an advection–diffusion equation, spatially centred using an Arakawa G-grid. Given the regional scale of the study and variability in diffusion terms along the coast, here, we ignored horizontal diffusion, thus focusing on the strength of advection in defining dispersal patterns (Largier, 2003). When the water depth was <1 m, particles were advected in 2-D. Concentrations of particles remained conservative over the model domain, with no behaviour implemented at the top, bottom and coastal boundaries. The offshore boundary was absorbing particles, but because of the spatial extent of the model, no particle ever reached that boundary. Since the present study focuses on the large-scale dispersal patterns and not on estimating absolute numbers of larval exchanges, the choice was made to consider particles as passive with no mortality rate included. Passive larval transport for a species-specific planktonic larval duration (PLD), for example, was found to be the dominant driver of gene flow (Padrón et al., 2018). Simulating dispersal of *S. alveolata* larvae in the western English Channel, Ayata et al. (2009) found that the number of settled larvae was inversely proportional to mortality rate (tested values ranged from 0 to 0.36 $day^{-1}$), but the dispersal

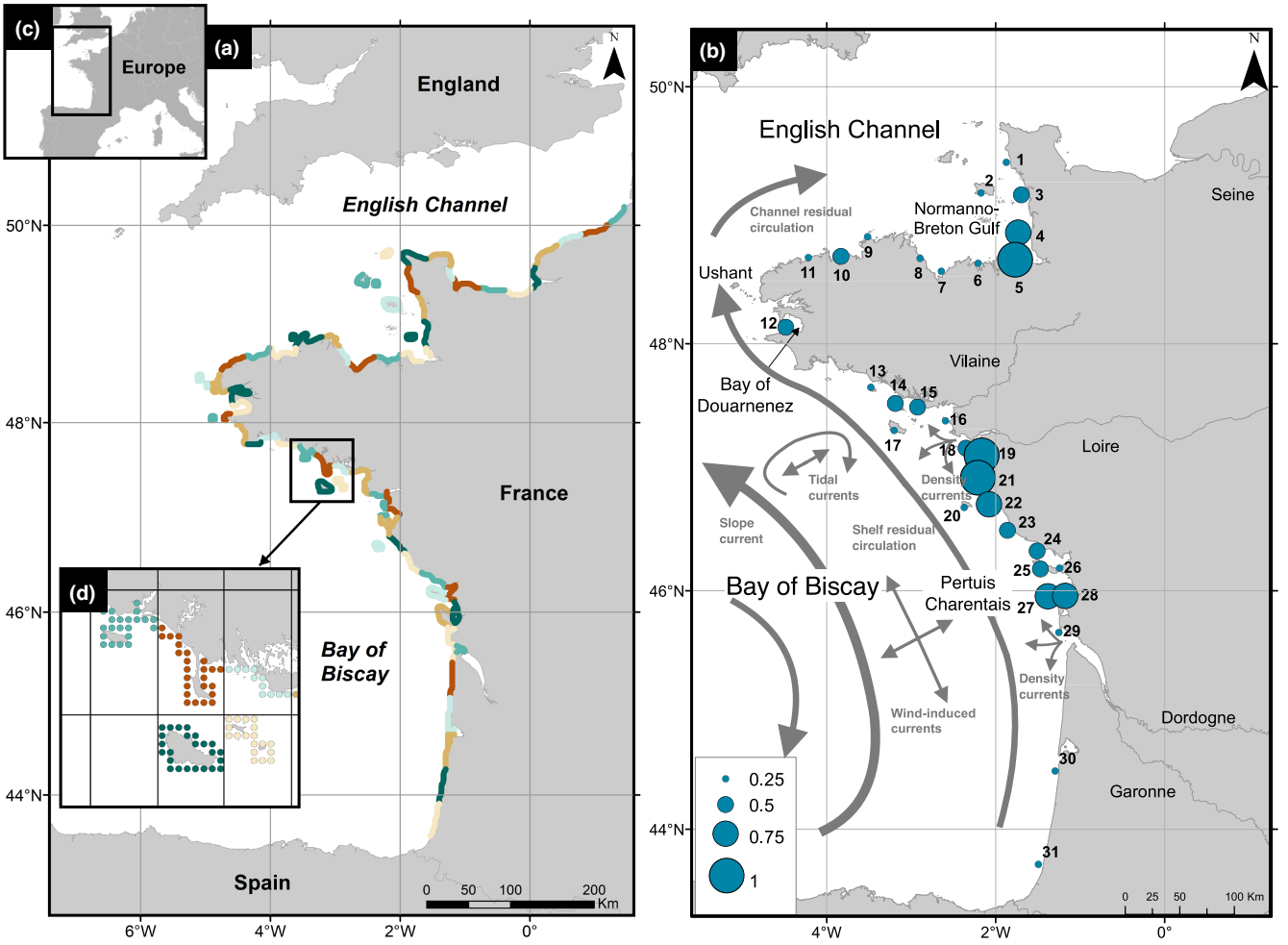


FIGURE 1 Study area located on the western coast of Europe (a, inset c). Coloured segments delineate distinct regional zones on the French Atlantic and Channel coastline considered to simulate hydrodynamic connectivity (a). The zones were delineated using a 30 km grid in which ocean model cells adjacent to coastline (indicated with coloured points in inset d) were pooled by individual zones. Among all the zones delineated along the coastline, only those containing *S. alveolata* reefs (numbered from 1 in the north to 31 in the south) were retained to analyse connectivity (b). Reef quality in each zone was characterized by Curd et al. (2020) using a semi-quantitative score (i.e., 0.25; 0.5; 0.75 or 1, as shown by bullet sizes). Arrows symbolize general ocean circulation patterns in the Bay of Biscay and the English Channel (after Ayata et al., 2010, based on Salomon & Breton, 1993, and Koutsikopoulos & Le Cann, 1996)

patterns and settlement dynamics were not altered. Nevertheless, we acknowledge the potential overestimation of connectivity levels by transport models, especially when mortality or vertical behaviour of larvae is not included (Manel et al., 2019; Paris et al., 2007). Setting the mortality coefficient to zero in transport models has the advantage of preserving potential, yet rare, dispersal events, while later back-calculating dispersal probabilities that include mortality can lead to exploring the more likely dispersal connections and pathways (Treml et al., 2008). Similar simplifications were considered in other studies on larval dispersal when the focus was on large-scale patterns (Álvarez-Noriega et al., 2020; Andrello et al., 2013) or on rare dispersal events (Treml et al., 2008).

Model outputs from the ocean and transport model, containing particles concentrations over the MARS3D model domain, were saved as netCDF files. The netCDF files were further analysed with the R software as follows. A 30 km×30 km horizontal grid was overlaid onto the MARS3D model grid to aggregate coastline ocean model cells into larger regional 'zones' covering the entire French Atlantic and Channel coastline (without *a priori* knowledge about reef occurrence and status within each zone) (Figure 1a, inset d). One zone grouped in average 21 MARS3D model cells of 2.5 km×2.5 km. The choice to aggregate model cells into larger zones was made in the attempt to get an overview of the broad-scale connectivity potential over the entire coast, as seen in other studies (Boschetti et al., 2020; Boulanger et al., 2020; Holstein et al., 2014). Our choice was based on the knowledge that large-scale oceanographic processes constrain small-scale processes, and thus are those that affect whether larvae are supplied near settlement sites (Pineda, 2000). We found the size of the coastal zones in our simulations to be representative of the dispersal kernel of *S. alveolata* larvae, which should be larger than the mean dispersal distance (Palumbi, 2003). In our simulations, larvae were transported over more than two adjacent zones at a time with no apparent overestimation in local retention, which could be indicative of too large zones (see Figure S1 in Appendix S1). Of the 60 zones covering the French

Atlantic and Channel coastline, only 31 contain recorded observations of *S. alveolata* reefs, and were considered ecologically relevant for the connectivity simulations (Figure 1b). Our choice of grid size reflects the best consensus we found between computational resources and the spatial scale and frequency of recorded observations of the species. Even with increased computational efforts due to higher-resolution modelling, a delineation of smaller zones would not have been feasible for our study for the simple reason that we lack the information on reef status and occupation in smaller grid cells. In the most comprehensive *S. alveolata* database (Curd et al., 2020), all known historical and contemporary records of the species presence and qualitative abundance were also polled into cells of 50 km (see figure at https://www.seanoe.org/data/00610/72164/) to provide an overview over the entire distribution domain of this species.

Simulations were initialized with particle concentrations of $10^6\,m^{-2}$ in the bottom layer of the model, assuming that homogenous densities of larvae are released from the seabed. Similar larval concentrations were estimated to be released by reefs in the Channel (Ayata et al., 2009), however, since we used relative connectivity rates throughout this study the effect of initial particle concentrations was insignificant. While in reality the release of larvae in the water takes place continuously over the spawning period of April to September (Dubois et al., 2007), here we chose for simplification to simulate several spawning events covering the seasonal variability, as commonly seen in other dispersal studies (Eriksen et al., 2020; Holstein et al., 2014; Vestfals et al., 2021). Specifically, larvae were released on the first day of the month over the *S. alveolata* spawning season, between the years 2012 and 2016, resulting in 27 simulations out of 30 (6 months × 5 years; three of the simulation runs gave errors and were thus excluded from the analysis). Over the simulated months and years, the first day of the month coincided with different moments of the tidal cycle, and therefore, was considered to cover tidal variability. Model simulations ran for 6 weeks (42 d), and particles dispersal outputs produced after 3, 4 and 6 weeks of dispersal, corresponding to in-situ estimates of *S. alveolata* PLD (Dubois et al., 2007). The model choices and assumptions regarding the size of the release zones, the spawning timing, lack of mortality or larval behaviour were made under practical constraints of computational feasibility of simulating large-scale connectivity and limited biological information. Running the ocean and transport model online with a small time-step, compared to many offline-coupled Lagrangian transport studies using daily mean circulation fields (e.g., Andrello et al., 2013; Holstein et al., 2014), was computationally expensive. This assured a better representation of large-scale advection processes over the study area (Largier, 2003), however, without making any inference on settlement dynamics where smaller-scale processes and larval behaviour prevail (Pineda et al., 2010).

## 2.3 | Hydrodynamic connectivity

At the end of each simulation, particle concentrations (labelled by the release or source zone) in each of the 31 geographic zones containing reefs were used to estimate connectivity patterns through three matrices as follows: (1) a connectivity matrix C, whose elements $c_{ij}$ represent the relative concentration of particles released in zone *i* found at the end of simulation in zone *j*; the diagonal, formed by the elements $c_{ii}$, represents the relative concentration of particles released in zone *i* found at the end of simulation in the same zone *i*, referred to as local retention; (2) an adjacent matrix A, derived from the connectivity matrix C based on a threshold (see Section on Network metrics and operations, link thresholding, for details), whose elements $a_{ij}$ have values of 0 if $c_{ij} <$ threshold, or 1 if $c_{ij} \geq$ threshold, corresponding to absence (0) or presence (1) of a connection between the zones *i* and *j*; and (3) a distance matrix D, whose elements $d_{ij}$ are linear distances in km between the geographic centre of zones *i* and *j* if the zones are connected ($a_{ij} = 1$), or are equal to zero if there is no connection ($a_{ij} = 0$). Linear geographic distance was applied between each two connected zones within either the Atlantic or the Channel. Because of the complex coastline configuration in the region, linear geographic distance between a Channel and an Atlantic zone would underestimate actual connectivity distance. As such, distance was calculated as the sum between the linear distance from the zone in the Channel to Ushant Island and the linear distance from Ushant Island to the zone on the Atlantic coast (Figure 1b). While transport of particles follows more dynamic patterns of coastal circulation than the linear geographic distance, which might indeed underestimate transport distance of individual particles (Andrello et al., 2013), the distance matrix D gives a measure of the minimum and direct geographic distance connecting two given zones, not the length of transport pathways. The coastline distance, on the other hand, might overestimate the connectivity distance in our case because of coastline topography with the presence of many islands, estuaries and bays in the study area. It needs to be mentioned that throughout the paper we are referring to larval dispersal, defined as the spread of larvae from a source area to a settlement site (considering only the start and end location), contrary to larval transport, which is longer than dispersal and follow the movement of larvae with ocean currents (Pineda et al., 2007). Therefore, we found the linear geographic distance to be representative in our case for larval dispersal estimates. This choice is also in line with the Eulerian transport used to estimate dispersal.

## 2.4 | Graphical representation of network connectivity

Graph theory (sensu Barabási, 2016) was used to explore patterns of connectivity in the network of reefs, identify zones with reefs of importance to network coherence, and indicate zones of concern or conservation priority. A 'graph' is the visual representation of a network of nodes connected by links, with each link $l_{ij}$ connecting two nodes $n_i$ and $n_j$ (Barabási, 2016; Urban & Keitt, 2001). In addition to direct links, there can be multiple ways to go from a node *i* to a node *j* (called 'paths'), passing by other nodes. The length of a path from $n_i$ to $n_j$ can be measured by the

number of links connecting the two nodes or the sum of their weights. Here, the nodes represent the coastal zones and were defined geographically using the spatial centroid of each zone (1–31; Figure 1b). Each node was *weighted* by a semi-quantitative score attributed to each zone, which was defined on expert knowledge and field observations on *S. alveolata* reefs, following the SACFOR scale (Superabundant, Abundant, Common, Frequent, Occasional, Rare) (Curd et al., 2020). The semi-quantitative scale was defined by the coverage of *S. alveolata* reefs in each zone, taking into account their spatial extension and their height: 0.25 for small reefs (Occasional, Rare), 0.5 for medium reefs (Frequent), 0.75 for large reefs (Common) and 1 for exceptionally large reefs (Superabundant, Abundant) (Figure 1b). Linkage weights were defined according to the three connectivity matrices described in the previous section as: (1) the relative connectivity between two nodes (matrix *C*); (2) the presence or absence of a connection (matrix *A*); and (3) the distance in km between connected zones (matrix *D*). The graph was constructed directionally, i.e., linkages account for the direction of larval transport from zone *i* to *j*, and weighted. The three connectivity measures attributed to linkage weights were alternatively used to estimate network metrics and operations, as detailed in the next section.

## 2.5 | Network metrics and operations

While there is a variety of metrics used in network analysis (Keeley et al., 2021), we selected here two simple and complementary metrics to characterize network structure: (1) the number of components, and (2) the relative size of the largest component. The number of components represents the number of disconnected (isolated) subgraphs, where a component is an isolated subgraph in which any two nodes are connected to each other by direct links or by paths but are unconnected to additional nodes either in the main graph or other isolated subgraphs. The relative size of the largest component represents the ratio between the number of nodes in the largest component of the graph (i.e., largest isolated subgraph) and the total number of nodes in the entire graph. Used together, these two metrics give a good overview of the fragmentation potential in a network (Urban & Keitt, 2001) which was of interest in this study. With this in mind, two types of operations were performed to examine connectedness and change in network structure following perturbation, such as losing one or more nodes and associated linkages, namely, link thresholding and node deletion (Urban & Keitt, 2001).

Link thresholding explores how the sequential constraining of links above a predetermined threshold alters the scale of connectivity and structure of the network (Treml et al., 2008). The threshold can be ecologically interpreted as the minimum relative flux of larvae required to effectively connect two distant sub-populations, and can be used to rescale connectivity (Cowen et al., 2006; Samsing et al., 2019; Treml et al., 2012). Below the threshold, larval flux is considered marginal, and the two sub-populations disconnected. As the threshold increases, the network gets fragmented into disconnected subgraphs (or components). It should be kept in mind that while this exercise will not reveal the exact levels of connectivity, it will allow a dynamic exploration of connectivity patterns and network coherence in absence of meaningful biological information. First, the network was built using the connectivity matrix *C* for linkage weights. Links were deleted from the network by iteratively increasing the threshold from zero (or no threshold applied in this case), which maintains all zones connected as a single component across all simulated spawning events, up to 7%, which results in each zone becoming an isolated or disconnected component (Figure S2). Link thresholding was performed across all simulated monthly and yearly spawning events ($N = 27$) and the number of components and the relative size of the largest component metrics were calculated. Second, the probability of network fragmentation was calculated as a probability matrix *F*, whose elements represent the presence probability of each link (*i*, *j*) across all simulated spawning events, estimated as the proportion of simulations for which the threshold was exceeded. In this case, the network was built using the information on the presence/absence of connections (adjacent matrix *A*) as linkages weight.

Node deletion tests the importance of individual zones to the coherence of the network by examining changes in network metrics following the removal of node(s). Here, we used a connectivity threshold of 0.0% to consider a fully connected network (as tested with link thresholding; Figure S2), where all zones are connected into one single component, at the beginning of each node deletion simulation. Nodes (and all associated links) were then deleted from the network iteratively using five different scenarios, i.e., 30 iterations (the total number of nodes in the network being 31) per scenario. Number of components and relative size of the largest component metrics were computed after each deletion until only one node remained. The five different scenarios used in node deletion are as follows:

1. *Random deletion*: nodes were randomly selected for each deletion event. For each sequential deletion ($N = 30$), a bootstrap approach was used to test for the effect of selecting a different node for deletion at each step. For each step, 125 permutations (a total of $30 \times 125 = 3750$ simulations) were run allowing mean metric estimates to be generated;
2. *Low betweenness centrality*: nodes were deleted starting with the smallest values in betweenness centrality metric $BC_i$ (Freeman, 1977). $BC_i$ measures the proportion of shortest paths *p* between any two nodes that pass through a focal node *i*. The shortest or fastest path $p_{jk}$ between two nodes *j* and *k*, here is the shortest distance (sum of linkages weight defined by the geographic linear distance in km, as in matrix *D*). The shortest path $p_{jk}$ was found using the Dijkstra's shortest path first algorithm in the directed and weighted graph (West, 1996). It is important to note that *BC* metric does not consider the number of direct paths, or links, of a node *i* in the graph, which represents the number of connections, nor the local retention $c_{ii}$, which represents a loop in the graph;

3. *High betweenness centrality*: nodes were deleted starting with the highest values in betweenness centrality metric $BC_i$ (see 2 above for definitions);
4. *Smallest reefs*: *in* ascending order, deleting each node based on the scale of reef quality (as shown in Figure 1d); and
5. *Largest reefs*: in descending order, deleting each node based on the scale of reef quality (as shown in Figure 1d).

Under Scenarios 4 and 5, in the event of ties in the scale of reef quality (there were 15 zones with a scale of 0.25, nine zones with 0.5, four zones with 0.75, and three zones with the maximal scale of 1), nodes were randomly removed and bootstrap simulations (125 permutations) performed as per Scenario 1.

Saved model outputs (netCDF files) from the ocean and transport model underwent post-processing in R, version 3.5.0 (R Core Team, 2020), specifically the particle concentrations in the coastal zones were extracted at the end of each run and connectivity matrices calculated. All network calculations and statistical analyses were undertaken using the *igraph* package (Csardi & Nepusz, 2006). Zone mapping was performed using ArcGIS version 10.6.1 (ESRI).

## 3 | RESULTS

### 3.1 | Link thresholding

The number of components in the network predictably increased with higher connectivity threshold values, while the relative size of the largest component decreased (Figure 2). At connectivity thresholds ≤0.01%, the network acted as a single component for all 3w, 4w and 6w PLDs (the mean over all simulations; Figure 2). Under a more conservative connectivity threshold of 0.05%, the network typically featured two components, with the largest component containing an average of 60% and 90% of the zones for a PLD of 3w and 4w, respectively (Figure 2). For a PLD of 6w the network remained connected into one component. Beyond this threshold, there was a relatively linear decrease/increase in relative size of the largest component/number of components. When a threshold of 0.5% was used, clear evidence of fragmentation of the network into four components was observed, notably occurring at the Bay of Douarnenez (Zone 12), indicating isolation of the Channel and Atlantic populations (Figures 2, 3 and S3). Comparison of linkage probabilities over all simulated spawning events between two thresholds confirms that at a threshold of 0.01% all zones are strongly connected into one compact network with medium to high probability. At a threshold of 0.5%, the network became fragmented into four components with low linkage probability among them (Figure 3 and S3). The absolute numbers of dispersing larvae and settlers are dependent on the production levels of local reefs, unknown for most *S. alveolata* reefs. Nevertheless, assessing relative connectivity potential (regardless of local spawning potential, as here we assumed homogeneous release of larvae) holds meaningful biological interpretation as these results strongly concur with the genetic structure of *S. alveolata* reefs. Nunes et al. (2021) showed that reefs along the Bay of Biscay and the English Channel were well connected within each region, but only little exchange seems to occur between the two regions. Hence, the genetic structure reflects a cut-off connectivity threshold resting between 0.01% and 0.5% for all PLDs tested of 3w, 4w or 6w. It should be noted that the threshold range found here meaningful remains descriptive for generic simulations of potential connectivity without larval behaviour, mortality or settlement rates. An attempt in applying a mortality rate of 0.09 $day^{-1}$ to dispersing larvae, as used by Ayata et al. (2009), would imply a daily exponential decrease in particle concentrations, resulting by the end of simulations to a remaining fraction of 0.15, 0.08 and 0.02 of the initial concentrations after 3w, 4w and 6w dispersal, respectively. In this case, the same fraction would reflect in a lower threshold inducing network fragmentation. Nevertheless, higher accumulated mortality over longer PLD would result in leveraging the differences in connectivity patterns resulted from various PLD by removing the longer and rare dispersal events.

### 3.2 | Node deletion

Among all scenarios, sequential deletion of zones starting with the *high betweenness centrality* (*highBC*) had the biggest impact on network fragmentation (Figures 4 and S4), hence those zones have the greatest influence on network structure and coherence. Taking the example of 4w PLD, which is a common PLD for this species (Dubois et al., 2007), the network fragmented into two disconnected components after just 5 node deletions. Deleting 10 (33%) nodes fragmented the original network into four components, with the largest component connecting ~1/3rd of all nodes. Sequential deletion of nodes based on reef size (smallest to largest reefs and vice versa) or random deletion of nodes were comparable (Figure 4). The same fragmentation patterns were obvious when 3w and 6w PLDs were tested, with slight variations in the magnitude of fragmentation (Figure S4). Nevertheless, by far, the nodes with *highBC* stand out as a meaningful criterion that needs to be considered in maintaining a connected network. Using a different threshold might shift the timing of fragmentation (equivalent here to the number of nodes deleted), but *highBC* would remain the most meaningful criterion among those (scenarios) tested here. The network retained its greatest coherence (i.e., as a single component) when sequentially deleting the *lowBC* nodes first (Figures 4 and S4). Because *lowBC* nodes are peripheral, their deletion did not fragment the network into disconnected components but rather gradually decreased the size of the largest component (Figure 4b). On the other hand, selecting the zones with the largest reefs for protection, which in general are considered the best source of larvae due to larger reproductive output, is not key in maintaining this network connected; nor is protecting the

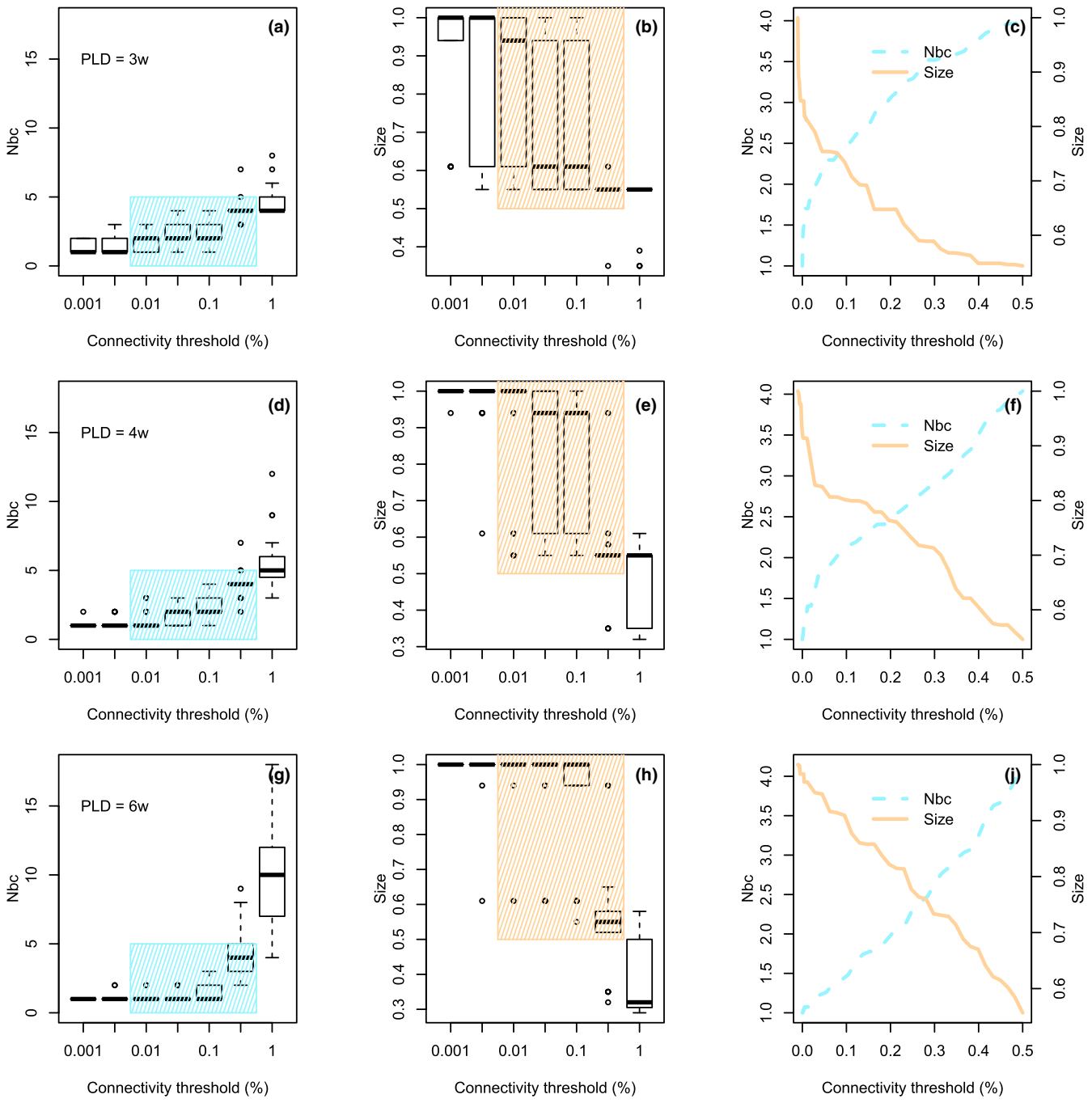


FIGURE 2 Change in network metrics number of components (Nbc; panels a, d, g) and relative size of the largest component (Size; panels b, e, h), under different connectivity thresholds (%). Data are pooled across all simulated spawning events with a pelagic larval duration of 3 (first row, panels a, b, c), 4 (second row, panels d, e, f) and 6 weeks (third row, panels g, h, j), and boxplots display median, 25% and 75% quantiles, and outliers. (c, f, j) Estimated mean change in network metrics (Nbc: Dashed blue line, Size: Solid orange line) are shown as a function of connectivity threshold values increasing from 0.01% (which implies that all zones are connected as a single component) to 0.5% (which implies that the network is fragmented into four components); mean values represent a subset of data highlighted with the blue (in panels a, d, g) and orange (in panels b, e, h) rectangles

smallest reefs, assuming those are at risk of extension. Indeed, adding more biological aspects to simulations, such as accurate estimations of reproductive output (or number of larvae released), mortality or settlement success rates, would increase the realism of simulations, but we remain confident that our key findings will not be altered.

## 4 | DISCUSSION

We used a biophysical model to simulate relative larval dispersal and assess connectivity potential among *S. alveolata* reefs along the French Atlantic and the Western English Channel coastline. Our results revealed a network of highly intra-connected reef

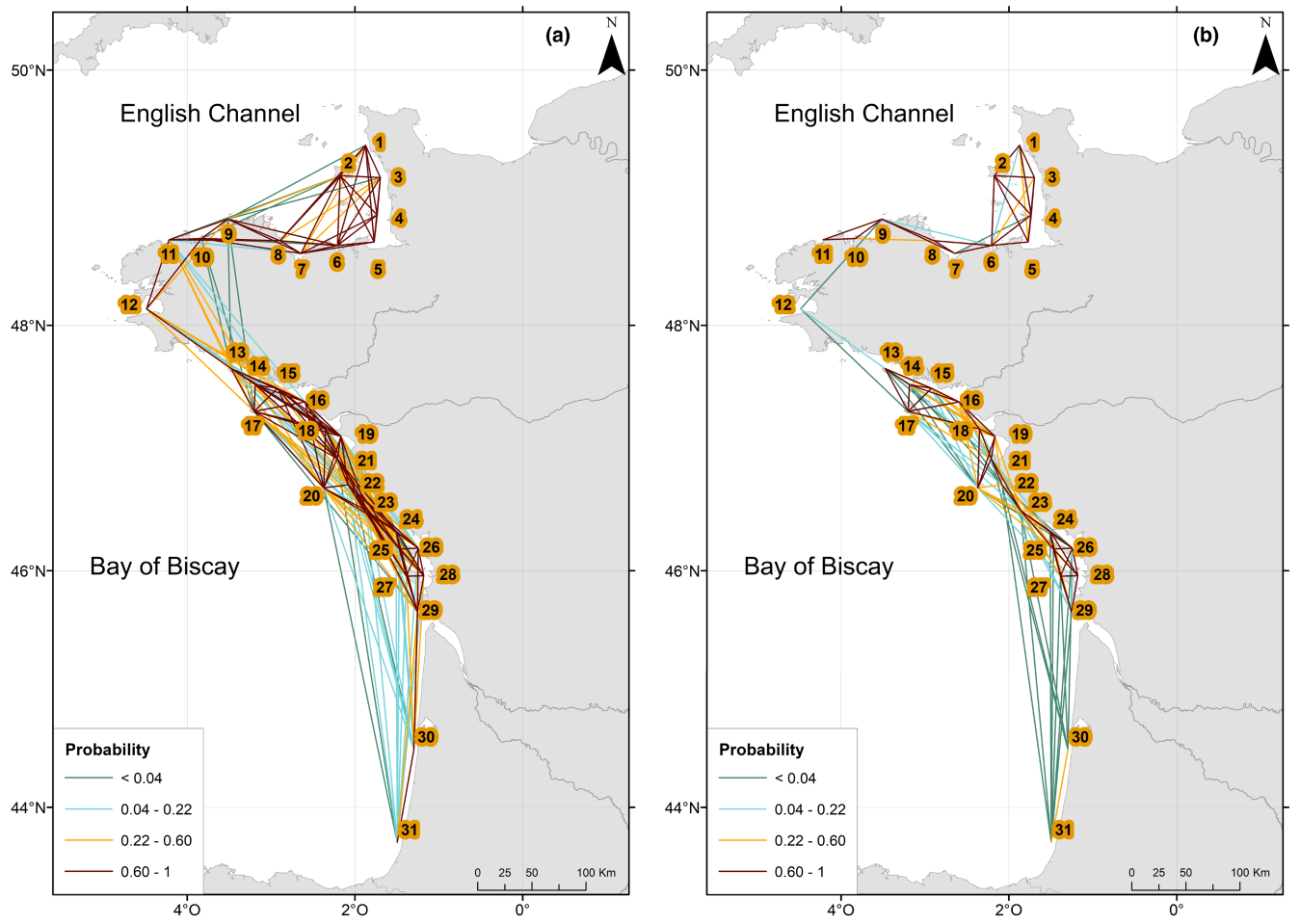


FIGURE 3 Network map showing the probability of a link between any two zones applying a connectivity threshold of 0.01% (a) and 0.5% (b). Probability is estimated as the presence frequency of a connection between two zones across all simulated spawning events with a pelagic larval duration of 4 weeks. The network is considered fragmented when the probability exceeds the arbitrarily set connectivity threshold (e.g., right map indicates 4 components: (1) zones 1–11; (2) zone 12; (3) zones 13–29; and (4) zones 30 and 31)

clusters linked through sporadic dispersal events. With limited biological features of the study species, link thresholding, an approach that in reality might reflect a reduction in the reproductive output (fecundity/patch size/quality), identified coastline locations most at risk of isolation from the wider network. On the other hand, reefs with high betweenness centrality were extremely important to network coherence and therefore should be the focus of conservation and/or protective measures to ensure metapopulation stability.

## 4.1 | Connectivity shapes metapopulation structure

Quantifying connectivity across seascapes, and specifically understanding how larval dispersal determines the strength and spatial structure of connectivity, is fundamental to understanding metapopulation structure (Treml et al., 2008). Our results suggest that the *S. alveolata* reefs along the Atlantic and English Channel coastlines of France resemble a 'small-world' network type (Watts & Strogatz, 1998) characterized by high connectivity among neighbouring zones over relatively short, linear steps. Similar network structures have been observed in coastal marine systems, including the Great Barrier Reef (Kininmonth et al., 2010) and the Southern California Bight (Watson et al., 2011), but also in other biological systems such as infectious diseases spread (Watts & Strogatz, 1998). Coastal marine populations are generally linked in a non-random fashion through larval dispersal with connectivity patterns constrained by coastline topography and oceanographic currents (Banks et al., 2007). When analysing the structure of networks, in addition to dispersal distances, connectivity strength is a key variable to be considered, varying from strong, permanent connections to weak, sporadic dispersal events among populations. Removing the weakest links in our simulated network on the French coast through link thresholding identified two distinct levels of connectivity: (1) highly interconnected reefs forming local clusters that were robust to link thresholding, and (2) weakly-linked regional clusters more sensitive to thresholding (and hence to reduction in larval transport) that can fragment the network into a number of isolated components. Even though our modelling assumptions may possibly have overestimated connectivity strength by not considering

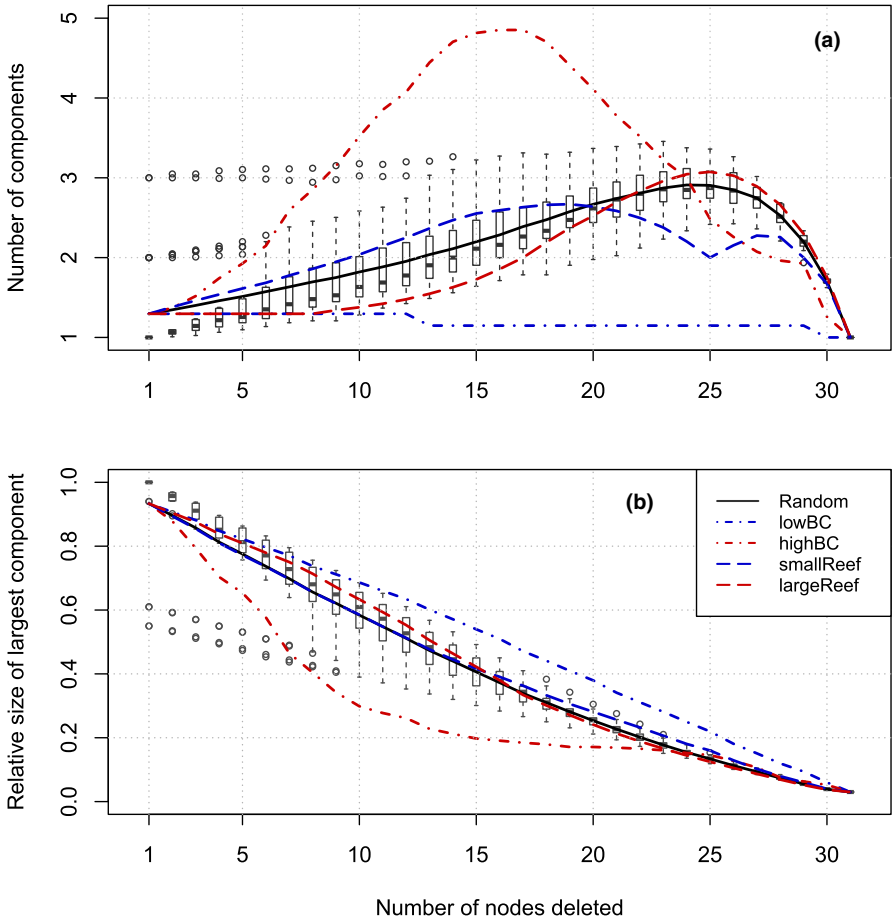


**FIGURE 4** Change in network metrics number of components (a) and relative size of the largest component (b), following sequential node deletion. Five node deletion scenarios were tested: (1) random deletion—Random; (1) sequential deletion of low to high betweenness centrality—lowBC; (3) sequential deletion of high to low betweenness centrality—highBC; (4) sequential deletion of the smallest to the largest reef—smallReef; and (5) sequential deletion of the largest to smallest reef—largeReef. For all node deletion tests, a total of 30 deletions were performed for each simulation and metrics recalculated after each deletion. An iterative approach was undertaken for the random deletion scenario and replicated (bootstrap without replacement) 125 times. Metrics were calculated on all simulated events with a pelagic larval duration of 4 weeks based on a connectivity threshold of 0.01%. The lines represent the average values of the two metrics for the simulated spawning events (Apr-Sep, 2012–2016). The grey boxplots show results from the random scenario across all replicates and the outliers with circles

mortality or settlement rates (Manel et al., 2019; Paris et al., 2007), the connectivity patterns observed remained robust over the range of thresholds and PLDs (3–6 weeks) tested. Thus, *S. alveolata* metapopulation (network) along the French coast is likely composed of clusters of reefs (i.e., Channel coast, Bay of Douarnenez, Atlantic coast, south of Gironde estuary) that are only inter-connected by occasional and marginal exchange of larvae.

The connectivity patterns shown here using hydrodynamic modelling are broadly consistent with other indirect measures of connectivity, based on genetic data collected for *S. alveolata* (Muir et al., 2020; Nunes et al., 2021). Genetic diversity and connectivity estimated with mitochondrial DNA (*cox-1* gene) and single nucleotide polymorphisms (SNPs) derived from nuclear DNA in *S. alveolata* across Europe show a strong genetic break between the Channel and the Atlantic coasts of France. This genetic break has also been observed in other marine invertebrates, whose populations depend on larval dispersal (Becquet et al., 2012; Nicolle et al., 2017), although some marine taxa do not present this differentiation (see examples in Maggs et al., 2008, Jenkins et al., 2018), suggesting that low connectivity between these two regions might be partially dependent on life-history traits, such as body size, larval behaviour and swimming ability (e.g. James et al., 2019; Jupe et al., 2020), affecting their capacity to overcome local hydrodynamic features. Genetic data also show some degree of differentiation among populations from the north and south of the Gironde estuary (Nunes et al., 2021), supporting our interpretation that the southern populations in the Bay of Biscay could be more isolated. It should be kept in mind that genetic differentiations among *S. alveolata* populations represent the realized connectivity (i.e., individuals successfully arrive in a new area and take part in reproduction), while hydrodynamic connectivity as simulated in our study represents the potential connectivity (i.e., individuals arrive in a new area but no further inference on their outcome is made) (Padrón et al., 2018).

Simulating hydrodynamic connectivity combined with network analysis as done here provides critical insights on metapopulation structure with only limited biological features of the study species. The suite of *S. alveolata* reefs considered in this region quickly transitions from a coherent single network into a fragmented multi-component network when a high connectivity threshold value was applied (simulating the loss of weak links). Applying a connectivity threshold of 0.5% led to near complete separation of the French Atlantic coast and Channel populations, although within these two regions, the network remains coherent indicating strong intra-regional connectivity. Genetic data support this finding, such that populations within the Channel or within the Atlantic are genetically homogeneous, indicating that gene flow within these two regions is broadly maintained (Muir et al., 2020; Nunes et al., 2021). Nevertheless, the low level of connectivity between these two regions, observed both in our model and in genetic studies, suggests that conservation management should be applied synergistically across both biogeographic regions. While sporadic long-distance exchange of individuals may maintain gene flow among regions, thereby reducing the level of endemism (Trakhtenbrot et al., 2005), such long-distance dispersal events may be too low to influence population dynamics (Burgess et al., 2014). To capture these rare dispersal events as identified by gene flow, it is thought necessary to use multigenerational modelling that integrates stepping-stone dispersal (Jahnke et al., 2018). In other contexts (e.g., metapopulation persistence, food webs), the importance of weak connections to network stability has previously been shown (Artzy-Randrup & Stone, 2010; Elton, 1927; Jahnke et al., 2018; Raffaelli, 2002). Our results similarly suggest that weak connections in this particular system are present and highly important to maintain gene flow (Manel et al., 2019; Nunes et al., 2021).

## 4.2 | Conservation management in a network of reefs

Simulations of network fragmentation help identify populations that significantly contribute to network coherence, either as central connectivity hubs or as pivotal stepping-stones between major network components (Barabási, 2016; Estrada & Bodin, 2008; Samsing et al., 2019). Our scenarios simulating sequential loss of reefs indicated that losing reefs in the zones with highest *betweenness centrality (BC)* resulted in a critical fragmentation of the network by removing as few as 5 nodes (considering a PLD of 4 weeks). Importantly, these areas located south of the Loire estuary that we identified as high *BC* zones, thus channelling many shortest connectivity paths between any other two reefs in the network, seemed to have been stable over the past decade, as they are colonized by some of the largest reef structures in Europe (Curd et al., 2020). Furthermore, these reefs are characterized by the highest genetic diversity among Atlantic *S. alveolata* reefs—another indication of large populations (Nunes et al., 2021), and are likely to contribute to wider metapopulation persistence acting as an important source of larvae to other reefs. Habitat suitability for *S. alveolata* is, however, predicted to significantly decline under future climate change scenarios (Curd et al., 2021), thus conservation efforts will be of critical importance to minimize local stressors and consolidate the resilience of these key connectivity hubs against anthropogenic- and climate-driven changes.

Stepping-stone reefs are, on the other hand, key for connecting distant populations otherwise disconnected, and represent disproportionately important linking pathways among discrete network components (Boulanger et al., 2020). For instance, network analysis identified the Bay of Douarnenez population at the most north-western tip of the French Atlantic coast as pivotal in connecting Atlantic and Channel populations and maintaining *S. alveolata* metapopulation coherence across the French western coast. However, the stepping-stone reefs identified in Bay of Douarnenez are hydrodynamically remote from major reef clusters and hence may be more at risk of becoming isolated from external larval supply. Effective protection of such important isolated reefs will rely on local conservation initiatives to minimize local stressors (e.g., trampling, Plicanti et al., 2016), but it also requires an in-depth understanding of larval exchange and local to regional hydrodynamics, so that networks can function in a way that sustains a combination of local reefs as well as connectivity paths among more distant reefs (Botsford et al., 2001; Cowen et al., 2007; Jones et al., 2007). As it can identify local zones that are critical to network coherence, betweenness centrality proves a relevant criterion to prevent network fragmentation in an effort to maintaining connectivity and biodiversity (Andrello et al., 2013; Estrada & Bodin, 2008; Holstein et al., 2014). Conversely, betweenness centrality proves just as relevant to induce network fragmentation, when spread of invasive species or parasites needs to be contained (Kölzsch & Blasius, 2011; Samsing et al., 2019). Either way, when network connectivity is at stake, betweenness centrality should therefore be considered by managers and decision makers in conservation and spatial planning.

## 4.3 | Adopting network analysis in conservation practice

Here, using a species of ecological and conservation importance, we have shown how combining hydrodynamic modelling and network analysis can be used to assess metapopulation structure and inform conservation management. In the first instance, the results represent an important yet previously overlooked first step in describing connectivity pathways among discrete populations of this protected species. This analysis can be relatively easily achieved using similar open-source modelling tools (van Sebille et al., 2018), established graph (network) packages (e.g., igraph), and bio-physical data describing the species and region of interest. Second, using basic network metrics and analyses, we identified reefs that are key to metapopulation functioning as contributing to

larval/recruitment pool and network coherence. The combination of larval dispersal modelling and network analysis can therefore be used to identify reefs for protection, monitoring or management interventions that are critical for network coherence, and to maintain large-scale connectivity. We argue that this approach alone is invaluable for describing connectivity pathways and network functioning with limited biological information. Further developments to integrate this connectivity modelling within a framework that also accounts for other population processes, such as recruitment timing and local population abundance, survivorship and fecundity, are nevertheless essential to further resolve different aspects of network structure as well as long-term metapopulation dynamics and persistence.

## ACKNOWLEDGEMENTS

This work is part of the REEHAB (REEf HABitat) project (www.honeycombworms.org), funded by the Total Foundation for the Biodiversity and the Sea (Grant No. 1512 215 588/F, 2015) and the Office Français de la Biodiversité (Carmen L David postdoctoral fellowship). The authors acknowledge the Pôle de Calcul et de Données Marines (PCDM) for providing DATARMOR (storage, data access, computational resources). We would like to thank Mathieu Caillaud, Benedict Thouvenin and Martin Plus for their support with the hydrodynamic model.

## CONFLICT OF INTEREST

The authors declare no competing interests.

## DATA AVAILABILITY STATEMENT

All input data and R code for data analysis are available on GitHub at https://github.com/cld321/connect_MARS3D.

## PEER REVIEW

The peer review history for this article is available at https://publons.com/publon/10.1111/ddi.13596.

## ORCID

*Carmen L. David* https://orcid.org/0000-0002-4241-1284
*Martin P. Marzloff* https://orcid.org/0000-0002-8152-4273
*Antony M. Knights* https://orcid.org/0000-0002-0916-3469
*Flávia L. D. Nunes* https://orcid.org/0000-0002-3947-6634
*Louise B. Firth* https://orcid.org/0000-0002-6620-8512
*Stanislas F. Dubois* https://orcid.org/0000-0002-3326-4892

## REFERENCES

Álvarez-Noriega, M., Burgess, S. C., Byers, J. E., Pringle, J. M., Wares, J. P., & Marshall, D. J. (2020). Global biogeography of marine dispersal potential. *Nature Ecology and Evolution*, *4*(9), 1196–1203. https://doi.org/10.1038/s41559-020-1238-y

Andrello, M., Mouillot, D., Beuvier, J., Albouy, C., Thuiller, W., & Manel, S. (2013). Low connectivity between Mediterranean marine protected areas: A biophysical modeling approach for the dusky grouper *Epinephelus marginatus*. *PLoS One*, *8*(7), e68564. https://doi.org/10.1371/journal.pone.0068564

Artzy-Randrup, Y., & Stone, L. (2010). Connectivity, cycles, and persistence thresholds in metapopulation networks. *PLoS Computational Biology*, *6*(8), e1000876. https://doi.org/10.1371/journal.pcbi.1000876

Ayata, S. D., Ellien, C., Dumas, F., Dubois, S., & Thiébaut, É. (2009). Modelling larval dispersal and settlement of the reef-building polychaete *Sabellaria alveolata*: Role of hydroclimatic processes on the sustainability of biogenic reefs. *Continental Shelf Research*, *29*(13), 1605–1623. https://doi.org/10.1016/j.csr.2009.05.002

Ayata, S. D., Lazure, P., & Thiébaut, É. (2010). How does the connectivity between populations mediate range limits of marine invertebrates? A case study of larval dispersal between the Bay of Biscay and the English Channel (North-East Atlantic). *Progress in Oceanography*, *87*(1–4), 18–36. https://doi.org/10.1016/j.pocean.2010.09.022

Banks, S. C., Piggott, M. P., Williamson, J. E., Bové, U., Holbrook, N. J., & Beheregaray, L. B. (2007). Oceanic variability and coastal topography shape genetic structure in a long-dispersing sea urchin. *Ecology*, *88*(12), 3055–3064. https://doi.org/10.1890/07-0091.1

Barabási, A. L. (2016). *Network science*. Cambridge University Press.

Beck, M. W., Brumbaugh, R. D., Airoldi, L., Carranza, A., Coen, L. D., Crawford, C., Defeo, O., Edgar, G. J., Hancock, B., Kay, M. C., Lenihan, H. S., Luckenbach, M. W., Toropova, C. L., Zhang, G., & Guo, X. (2011). Oyster reefs at risk and recommendations for conservation, restoration and management. *Bioscience*, *61*(2), 107–116. https://doi.org/10.1525/bio.2011.61.2.5

Becquet, V., Simon-Bouhet, B., Pante, E., Hummel, H., & Garcia, P. (2012). Glacial refugium versus range limit: Conservation genetics of *Macoma balthica*, a key species in the Bay of Biscay (France). *Journal of Experimental Marine Biology and Ecology*, *432–433*, 73–82. https://doi.org/10.1016/j.jembe.2012.07.008

Bertocci, I., Badalamenti, F., Lo Brutto, S., Mikac, B., Pipitone, C., Schimmenti, E., Vega Fernández, T., & Musco, L. (2017). Reducing the data-deficiency of threatened European habitats: Spatial variation of sabellariid worm reefs and associated fauna in the Sicily Channel, Mediterranean Sea. *Marine Environmental Research*, *130*, 325–337. https://doi.org/10.1016/j.marenvres.2017.08.008

Bishop, M. J., Mayer-Pinto, M., Airoldi, L., Firth, L. B., Morris, R. L., Loke, L. H. L., Hawkins, S. J., Naylor, L. A., Coleman, R. A., Chee, S. Y., & Dafforn, K. A. (2017). Effects of ocean sprawl on ecological connectivity: Impacts and solutions. *Journal of Experimental Marine Biology and Ecology*, *492*, 7–30. https://doi.org/10.1016/j.jembe.2017.01.021

Bodin, Ö., & Saura, S. (2010). Ranking individual habitat patches as connectivity providers: Integrating network analysis and patch removal experiments. *Ecological Modelling*, *221*(19), 2393–2405. https://doi.org/10.1016/J.ECOLMODEL.2010.06.017

Boschetti, F., Babcock, R. C., Doropoulos, C., Thomson, D. P., Feng, M., Slawinski, D., Berry, O., & Vanderklift, M. A. (2020). Setting priorities for conservation at the interface between ocean circulation, connectivity, and population dynamics. *Ecological Applications*, *30*(1), e02011. https://doi.org/10.1002/eap.2011

Botsford, L. W., Hastings, A., & Gaines, S. D. (2001). Dependence of sustainability on the configuration of marine reserves and larval dispersal distance. *Ecology Letters*, *4*(2), 144–150. https://doi.org/10.1046/j.1461-0248.2001.00208.x

Boulanger, E., Dalongeville, A., Andrello, M., Mouillot, D., & Manel, S. (2020). Spatial graphs highlight how multi-generational dispersal shapes landscape genetic patterns. *Ecography*, *43*(8), 1167–1179. https://doi.org/10.1111/ecog.05024

Le Boyer, A., Charria, G., Le Cann, B., Lazure, P., & Marié, L. (2013). Circulation on the shelf and the upper slope of the Bay of Biscay. *Continental Shelf Research*, *55*, 97–107. https://doi.org/10.1016/j.csr.2013.01.006

Le Bris, A., Fréchet, A., & Wroblewski, J. S. (2013). Supplementing electronic tagging with conventional tagging to redesign fishery closed

areas. *Fisheries Research*, *148*, 106–116. https://doi.org/10.1016/j.fishres.2013.08.013

Bunn, A. G., Urban, D. L., & Keitt, T. H. (2000). Landscape connectivity: A conservation application of graph theory. *Journal of Environmental Management*, *59*(4), 265–278. https://doi.org/10.1006/JEMA.2000.0373

Burgess, S. C., Nickols, K. J., Griesemer, C., Barnett, L. A. K., Dedrick, A. G., Satterthwaite, E. V., Yamane, L., Morgan, S. G., White, J. W., & Bostford, L. W. (2014). Beyond connectivity: How empirical methods can quantify population persistence to improve marine protected area design. *Ecological Society of America*, *24*(2), 8–270. https://doi.org/10.1890/13-0710.1

Chaverra, A., Wieters, E., Foggo, A., & Knights, A. M. (2019). Removal of intertidal grazers by human harvesting leads to alteration of species interactions, community structure and resilience to climate change. *Marine Environmental Research*, *146*, 57–65. https://doi.org/10.1016/j.marenvres.2019.03.003

Cowen, R. K., Gawarkiewicz, G., Pineda, J., Thorrold, S. R., & Werner, F. E. (2007). Population connectivity in marine systems an overview. *Oceanography*, *20*, 14–21. https://doi.org/10.2307/24860093

Cowen, R. K., Paris, C. B., & Srinivasan, A. (2006). Scaling of connectivity in marine populations. *Science*, *311*(5760), 522–527. https://doi.org/10.1126/science.1122039

Cowen, R. K., & Sponaugle, S. (2009). Larval dispersal and marine population connectivity. *Annual Review of Marine Science*, *1*(1), 443–466. https://doi.org/10.1146/annurev.marine.010908.163757

Csardi, G., & Nepusz, T. (2006). The igraph software package for complex network research. *Inter Journal Complex Systems*, *1695*, 1–9.

Curd, A., Boyé, A., Cordier, C., Pernet, F., Firth, L. B., Bush, L. E., Davies, A. J., Lima, F. P., Meneghesso, C., Quéré, C., Seabra, R., Vasquez, M., & Dubois, S. F. (2021). Environmental optima for an ecosystem engineer: A multidisciplinary trait-based approach. *Scientific Reports*, *11*(1), 1–12. https://doi.org/10.1038/s41598-021-02351-7

Curd, A., Cordier, C., Firth, L. B., Bush, L., Gruet, Y., Le, M. P., Blaze, J. A., Board, C., Bordeyne, F., Burrows, M. T., et al. (2020). *A broad-scale long-term dataset of Sabellaria alveolata distribution and abundance curated through the REEHAB (REEf HABitat) project*. SEANOE. https://doi.org/10.17882/72164

Dubois, S., Commito, J. A., Olivier, F., & Retière, C. (2006). Effects of epibionts on *Sabellaria alveolata* (L.) biogenic reefs and their associated fauna in the bay of Mont saint-Michel. *Estuarine, Coastal and Shelf Science*, *68*(3–4), 635–646. https://doi.org/10.1016/j.ecss.2006.03.010

Dubois, S., Comtet, T., Retière, C., & Thiébaut, E. (2007). Distribution and retention of *Sabellaria alveolata* larvae (Polychaeta: Sabellariidae) in the bay of Mont-saint-Michel, France. *Marine Ecology Progress Series*, *346*(1), 243–254. https://doi.org/10.3354/meps07011

Dubois, S., Retière, C., & Olivier, F. (2002). Biodiversity associated with *Sabellaria alveolata* (Polychaeta: Sabellariidae) reefs: Effects of human disturbances. *Journal of the Marine Biological Association of the United Kingdom*, *82*(5), 817–826. https://doi.org/10.1017/S0025315402006185

Elton, C. S. (1927). *Animal ecology*. Sidgwick & Jackson.

Eriksen, E., Huserbråten, M., Gjøsæter, H., Vikebø, F., & Albretsen, J. (2020). Polar cod egg and larval drift patterns in the Svalbard archipelago. *Polar Biology*, *43*, 1–14. https://doi.org/10.1007/s00300-019-02549-6

Estrada, E., & Bodin, Ö. (2008). Using network centrality measures to manage landscape connectivity. *Ecological Applications*, *18*(7), 1810–1825. https://doi.org/10.1890/07-1419.1

Firth, L. B., Curd, A., Hawkins, S. J., Knights, A. M., Blaze, J. A., Burrows, M. T., Dubois, S. F., Edwards, H., Foggo, A., Gribben, P. E., Grant, L., Harris, D., Mieszkowska, N., Nunes, F. L. D., Nunn, J. D., Power, A. M., O'Riordan, R. M., McGrath, D., Simkanin, C., & O'Connor, N. E. (2021a). On the diversity and distribution of a data deficient habitat in a poorly mapped region: The case of *Sabellaria alveolata* L. in Ireland. *Marine Environmental Research*, *169*, 105344. https://doi.org/10.1016/j.marenvres.2021.105344

Firth, L. B., Harris, D., Blaze, J. A., Marzloff, M. P., Boyé, A., Miller, P. I., Curd, A., Vasquez, M., Nunn, J. D., O'Connor, N. E., et al. (2021b). Specific niche requirements underpin multidecadal range edge stability, but may introduce barriers for climate change adaptation. *Diversity and Distributions*, *27*(4), 668–683. https://doi.org/10.1111/ddi.13224

Firth, L. B., Knights, A. M., Bridger, D., Evans, A., Mieskowska, N., Moore, P. J., O'Connor, N. E., Sheehan, E. V., Thompson, R. C., & Hawkins, S. J. (2016). Ocean sprawl: Challenges and opportunities for biodiversity management in a changing world. *Oceanography and Marine Biology*, *54*, 193–269.

Firth, L. B., Mieszkowska, N., Grant, L. M., Bush, L. E., Davies, A. J., Frost, M. T., Moschella, P. S., Burrows, M. T., Cunningham, P. N., Dye, S. R., & Hawkins, S. J. (2015). Historical comparisons reveal multiple drivers of decadal change of an ecosystem engineer at the range edge. *Ecology and Evolution*, *5*(15), 3210–3222. https://doi.org/10.1002/ece3.1556

Freeman, L. C. (1977). A set of measures of centrality based on betweenness. *Sociometry*, *40*(1), 35. https://doi.org/10.2307/3033543

Gaggiotti, O. E., Brooks, S. P., Amos, W., & Harwood, J. (2004). Combining demographic, environmental and genetic data to test hypotheses about colonization events in metapopulations. *Molecular Ecology*, *13*(4), 811–825. https://doi.org/10.1046/j.1365-294X.2003.02028.x

van Gennip, S. J., Popova, E. E., Yool, A., Pecl, G. T., Hobday, A. J., & Sorte, C. J. B. (2017). Going with the flow: The role of ocean circulation in global marine ecosystems under a changing climate. *Global Change Biology*, *23*(7), 2602–2617. https://doi.org/10.1111/gcb.13586

Gonzalez, A., Thompson, P., & Loreau, M. (2017). Spatial ecological networks: Planning for sustainability in the long-term. *Current Opinion in Environmental Sustainability*, *29*, 187–197. https://doi.org/10.1016/j.cosust.2018.03.012

Hastings, A., & Botsford, L. W. (2006). Persistence of spatial populations depends on returning home. *Proceedings of the National Academy of Sciences of the United States of America*, *103*(15), 6067–6072. https://doi.org/10.1073/pnas.0506651103

Holstein, D., Paris, C., & Mumby, P. (2014). Consistency and inconsistency in multispecies population network dynamics of coral reef ecosystems. *Marine Ecology Progress Series*, *499*, 1–18. https://doi.org/10.3354/meps10647

Huret, M., Petitgas, P., & Woillez, M. (2010). Dispersal kernels and their drivers captured with a hydrodynamic model and spatial indices: A case study on anchovy (*Engraulis encrasicolus*) early life stages in the Bay of Biscay. *Progress in Oceanography*, *87*(1–4), 6–17. https://doi.org/10.1016/j.pocean.2010.09.023

Jahnke, M., Jonsson, P. R., Moksnes, P. O., Loo, L. O., Nilsson Jacobi, M., & Olsen, J. L. (2018). Seascape genetics and biophysical connectivity modelling support conservation of the seagrass *Zostera marina* in the Skagerrak–Kattegat region of the eastern North Sea. *Evolutionary Applications*, *11*(5), 645–661. https://doi.org/10.1111/eva.12589

James, M. K., Polton, J. A., Brereton, A. R., Howell, K. L., Nimmo-Smith, W. A. M., & Knights, A. M. (2019). Reverse engineering field-derived vertical distribution profiles to infer larval swimming behaviors. *Proceedings of the National Academy of Sciences of the United States of America*, *116*(24), 11818–11823. https://doi.org/10.1073/pnas.1900238116

Jenkins, T. L., Castilho, R., & Stevens, J. R. (2018). Meta-analysis of Northeast Atlantic marine taxa shows contrasting phylogeographic patterns following post-LGM expansions. *PeerJ*, *2018*(9), e5684. https://doi.org/10.7717/peerj.5684

Jones, A. G., Dubois, S. F., Desroy, N., & Fournier, J. (2018). Interplay between abiotic factors and species assemblages mediated by the

ecosystem engineer *Sabellaria alveolata* (Annelida: Polychaeta). *Estuarine, Coastal and Shelf Science*, *200*, 1–18. https://doi.org/10.1016/J.ECSS.2017.10.001

Jones, G., Srinivasan, M., & Almany, G. (2007). Population connectivity and conservation of marine biodiversity. *Oceanography*, *20*(3), 100–111. https://doi.org/10.5670/oceanog.2007.33

Jupe, L. L., Bilton, D. T., & Knights, A. M. (2020). Do differences in developmental mode shape the potential for local adaptation? *Ecology*, *101*(3), e02942. https://doi.org/10.1002/ecy.2942

Keeley, A. T. H., Beier, P., & Jenness, J. S. (2021). Connectivity metrics for conservation planning and monitoring. *Biological Conservation*, *255*, 109008. https://doi.org/10.1016/j.biocon.2021.109008

Kelly-Gerreyn, B. A., Hydes, D. J., Jégou, A. M., Lazure, P., Fernand, L. J., Puillat, I., & Garcia-Soto, C. (2006). Low salinity intrusions in the western English Channel. *Continental Shelf Research*, *26*(11), 1241–1257. https://doi.org/10.1016/j.csr.2006.03.007

Kininmonth, S. J., Déath, G., & Possingham, H. P. (2010). Graph theoretic topology of the great but small barrier reef world. *Theoretical Ecology*, *3*(2), 75–88. https://doi.org/10.1007/s12080-009-0055-3

Knights, A. M., Crowe, T. P., & Burnell, G. (2006). Mechanisms of larval transport: Vertical distribution of bivalve larvae varies with tidal conditions. *Marine Ecology Progress Series*, *326*, 167–174. https://doi.org/10.3354/meps326167

Knights, A. M., Culhane, F., Hussain, S. S., Papadopoulou, K. N., Piet, G. J., Raakær, J., Rogers, S. I., & Robinson, L. A. (2014). A step-wise process of decision-making under uncertainty when implementing environmental policy. *Environmental Science and Policy*, *39*, 56–64. https://doi.org/10.1016/j.envsci.2014.02.010

Kölzsch, A., & Blasius, B. (2011). Indications of marine bioinvasion from network theory: An analysis of the global cargo ship network. *European Physical Journal B*, *84*(4), 601–612. https://doi.org/10.1140/epjb/e2011-20228-5

Koutsikopoulos, C., & Le Cann, B. (1996). Physical processes and hydrological structures related to the Bay of Biscay anchovy. *Scientia Marina*, *60*, 9–19.

Largier, J. L. (2003). Considerations in estimating larval dispersal distances from oceanographic data. *Ecological Applications*, *13*(1 Suppl), 71–89. https://doi.org/10.1890/1051-0761(2003)013[0071:cield]2.0.co;2

Lazure, P., & Dumas, F. (2008). An external-internal mode coupling for a 3D hydrodynamical model for applications at regional scale (MARS). *Advances in Water Resources*, *31*(2), 233–250. https://doi.org/10.1016/j.advwatres.2007.06.010

Lazure, P., Garnier, V., Dumas, F., Herry, C., & Chifflet, M. (2009). Development of a hydrodynamic model of the Bay of Biscay. Validation of hydrology. *Continental Shelf Research*, *29*(8), 985–997. https://doi.org/10.1016/j.csr.2008.12.017

Lemasson, A. J., Fletcher, S., Hall-Spencer, J. M., & Knights, A. M. (2017). Linking the biological impacts of ocean acidification on oysters to changes in ecosystem services: A review. *Journal of Experimental Marine Biology and Ecology*, *492*, 49–62. https://doi.org/10.1016/j.jembe.2017.01.019

Liggins, L., Treml, E. A., & Riginos, C. (2013). Taking the plunge: An introduction to undertaking seascape genetic studies and using biophysical models. *Geography Compass*, *7*(3), 173–196. https://doi.org/10.1111/gec3.12031

Maggs, C. A., Castilho, R., Foltz, D., Henzler, C., Jolly, M. T., Kelly, J., Olsen, J., Perez, K. E., Stam, W., Väinölä, R., Viard, F., & Wares, J. (2008). Evaluating signatures of glacial refugia for North Atlantic benthic marine taxa. *Ecology*, *89*(1 Suppl), S108–S122. https://doi.org/10.1890/08-0257.1

Manel, S., Loiseau, N., & Puebla, O. (2019). Long-distance marine connectivity: Poorly understood but potentially important. *Trends in Ecology & Evolution*, *34*(8), 688–689. https://doi.org/10.1016/j.tree.2019.05.011

Ménesguen, A., Dussauze, M., Dumas, F., Thouvenin, B., Garnier, V., Lecornu, F., & Répécaud, M. (2019). Ecological model of the Bay of Biscay and English Channel shelf for environmental status assessment part 1: Nutrients, phytoplankton and oxygen. *Ocean Modelling*, *133*, 56–78. https://doi.org/10.1016/j.ocemod.2018.11.002

Muir, A. P., Dubois, S. F., Ross, R. E., Firth, L. B., Knights, A. M., Lima, F. P., Seabra, R., Corre, E., Le Corguillé, G., & Nunes, F. L. D. (2020). Seascape genomics reveals population isolation in the reef-building honeycomb worm, *Sabellaria alveolata* (L.). *BMC Evolutionary Biology*, *20*(1), 100. https://doi.org/10.1186/s12862-020-01658-9

Nicolle, A., Moitié, R., Ogor, J., Dumas, F., Foveau, A., Foucher, E., & Thiébaut, E. (2017). Modelling larval dispersal of *Pecten maximus* in the English Channel: A tool for the spatial management of the stocks. *ICES Journal of Marine Science*, *74*(6), 1812–1825. https://doi.org/10.1093/icesjms/fsw207

Noernberg, M. A., Fournier, J., Dubois, S., & Populus, J. (2010). Using airborne laser altimetry to estimate *Sabellaria alveolata* (Polychaeta: Sabellariidae) reefs volume in tidal flat environments. *Estuarine, Coastal and Shelf Science*, *90*(2), 93–102. https://doi.org/10.1016/j.ecss.2010.07.014

North, E. W., Gallego, A., & Petitgas, P. (2009). *Manual of recommended practices for modelling physical–biological interactions during fish early life*. ICES Cooperative Research Report **295**. International Council for the Exploration of the Sea (ICES).

Nunes, F. L. D., Rigal, F., Dubois, S. F., & Viard, F. (2021). Looking for diversity in all the right places? Genetic diversity is highest in peripheral populations of the reef-building polychaete *Sabellaria alveolata*. *Marine Biology*, *168*(5), 1–16. https://doi.org/10.1007/s00227-021-03861-8

Padrón, M., Costantini, F., Baksay, S., Bramanti, L., & Guizien, K. (2018). Passive larval transport explains recent gene flow in a Mediterranean gorgonian. *Coral Reefs*, *37*(2), 495–506. https://doi.org/10.1007/s00338-018-1674-1

Palumbi, S. R. (2003). Population genetics, demographic connectivity, and the design of marine reserves. *Ecological Applications*, *13*(sp1), 146–158. https://doi.org/10.1890/1051-0761(2003)013[0146:PGDCAT]2.0.CO;2

Paris, C. B., Chérubin, L. M., & Cowen, R. K. (2007). Surfing, spinning, or diving from reef to reef: Effects on population connectivity. *Marine Ecology Progress Series*, *347*, 285–300. https://doi.org/10.3354/meps06985

Patterson, S., & Bamieh, B. (2014). Consensus and coherence in fractal networks. *IEEE Transactions on Control of Network Systems*, *1*(4), 338–348. https://doi.org/10.1109/TCNS.2014.2357552

Piet, G. J., Jongbloed, R. H., Knights, A. M., Tamis, J. E., Paijmans, A. J., van der Sluis, M. T., de Vries, P., & Robinson, L. A. (2015). Evaluation of ecosystem-based marine management strategies based on risk assessment. *Biological Conservation*, *186*, 158–166. https://doi.org/10.1016/j.biocon.2015.03.011

Pineda, J. (2000). Linking larval settlement to larval transport: Assumptions, potentials, and pitfalls. *Oceanography of the Eastern Pacific*, *1*, 84–105.

Pineda, J., Hare, J., & Sponaugle, S. (2007). Larval transport and dispersal in the coastal ocean and consequences for population connectivity. *Oceanography*, *20*(3), 22–39. https://doi.org/10.5670/oceanog.2007.27

Pineda, J., Porri, F., Starczak, V., & Blythe, J. (2010). Causes of decoupling between larval supply and settlement and consequences for understanding recruitment and population connectivity. *Journal of Experimental Marine Biology and Ecology*, *392*, 9–21. https://doi.org/10.1016/j.jembe.2010.04.008

Plicanti, A., Domínguez, R., Dubois, S. F., & Bertocci, I. (2016). Human impacts on biogenic habitats: Effects of experimental trampling on *Sabellaria alveolata* (Linnaeus, 1767) reefs. *Journal of Experimental Marine Biology and Ecology*, *478*, 34–44. https://doi.org/10.1016/J.JEMBE.2016.02.001

R Core Team. (2020). *R: A language and environment for statistical computing*. R Foundation for Statistical Computing https://www.r-project.org/

Raffaelli, D. (2002). From Elton to mathematics and back again. *Science*, *296*(5570), 1035–1037. https://doi.org/10.1126/science.1072080

Salomon, J. C., & Breton, M. (1993). An atlas of long-term currents in the channel. *Oceanologica Acta*, *16*, 439–448.

Samsing, F., Johnsen, I., Treml, E. A., & Dempster, T. (2019). Identifying 'firebreaks' to fragment dispersal networks of a marine parasite. *International Journal for Parasitology*, *49*(3–4), 277–286. https://doi.org/10.1016/j.ijpara.2018.11.005

van Sebille, E., Griffies, S. M., Abernathey, R., Adams, T. P., Berloff, P., Biastoch, A., Blanke, B., Chassignet, E. P., Cheng, Y., Cotter, C. J., Deleersnijder, E., Döös, K., Drake, H. F., Drijfhout, S., Gary, S. F., Heemink, A. W., Kjellsson, J., Koszalka, I. M., Lange, M., … Zika, J. D. (2018). Lagrangian Ocean analysis: Fundamentals and practices. *Ocean Modelling*, *121*, 49–75. https://doi.org/10.1016/j.ocemod.2017.11.008

Shanks, A. L., Grantham, B. A., & Carr, M. H. (2003). Propagule dispersal distance and the size and spacing of marine reserves. *Ecological Applications*, *13*(1 Suppl), 159–169. https://doi.org/10.1890/1051-0761(2003)013[0159:pddats]2.0.co;2

Shin, S.-I., & Alexander, M. A. (2020). Dynamical downscaling of future hydrographic changes over the Northwest Atlantic Ocean. *Journal of Climate*, *33*(7), 2871–2890. https://doi.org/10.1175/jcli-d-19-0483.1

Spalding, M. D., Fox, H. E., Allen, G. R., Davidson, N., Ferdaña, Z. A., Finlayson, M., Halpern, B. S., Jorge, M. A., Lombana, A., Lourie, S. A., Martin, K. D., McManus, E., Molnar, J., Recchia, C. A., & Robertson, J. (2007). Marine ecoregions of the world: A bioregionalization of coastal and shelf areas. *Bioscience*, *57*(7), 573–583. https://doi.org/10.1641/B570707

Trakhtenbrot, A., Nathan, R., Perry, G., & Richardson, D. M. (2005). The importance of long-distance dispersal in biodiversity conservation. *Diversity and Distributions*, *11*(2), 173–181. https://doi.org/10.1111/j.1366-9516.2005.00156.x

Treml, E. A., Halpin, P. N., Urban, D. L., & Pratson, L. F. (2008). Modeling population connectivity by ocean currents, a graph-theoretic approach for marine conservation. *Landscape Ecology*, *23*(S1), 19–36. https://doi.org/10.1007/s10980-007-9138-y

Treml, E. A., Roberts, J. J., Chao, Y., Halpin, P. N., Possingham, H. P., & Riginos, C. (2012). Reproductive output and duration of the pelagic larval stage determine seascape-wide connectivity of marine populations. *Integrative and Comparative Biology*, *52*(4), 525–537. https://doi.org/10.1093/icb/ics101

Urban, D. L., & Keitt, T. (2001). Landscape connectivity: A graph-theoretic perspective. *Ecology*, *82*(5), 1205–1218. https://doi.org/10.1890/0012-9658(2001)082[1205:LCAGTP]2.0.CO;2

Urban, D. L., Minor, E. S., Treml, E. A., & Schick, R. S. (2009). Graph models of habitat mosaics. *Ecology Letters*, *12*(3), 260–273. https://doi.org/10.1111/j.1461-0248.2008.01271.x

Vestfals, C. D., Mueter, F. J., Hedstrom, K. S., Laurel, B. J., Petrik, C. M., Duffy-Anderson, J. T., & Danielson, S. L. (2021). Modeling the dispersal of polar cod (*Boreogadus saida*) and saffron cod (*Eleginus gracilis*) early life stages in the Pacific Arctic using a biophysical transport model. *Progress in Oceanography*, *196*, 102571. https://doi.org/10.1016/j.pocean.2021.102571

Watson, J. R., Siegel, D. A., Kendall, B. E., Mitarai, S., Rassweiller, A., & Gaines, S. D. (2011). Identifying critical regions in small-world marine metapopulations. *Proceedings of the National Academy of Sciences of the United States of America*, *108*(43), E907–E913. https://doi.org/10.1073/pnas.1111461108

Watts, D. J., & Strogatz, S. H. (1998). Collective dynamics of "small-world" networks. *Nature*, *393*(6684), 440–442. https://doi.org/10.1038/30918

West, D. B. (1996). *Introduction to graph theory*. Prentice Hall.

Wilson, D. P. (1970). Additional observations on larval growth and settlement of *Sabellaria alveolata*. *Journal of the Marine Biological Association of the United Kingdom*, *50*, 1–31.

## BIOSKETCH

The research team is part of the REEHAB (REEf HABitat) project (www.honeycombworms.org), which was launched in 2016 as an international collaborative research on the *Sabellaria alveaolta* biogenic reefs. The members of the research team are focused on assessing the ecological status of the reefs across their distributional range, developing a monitoring health index, and providing science-based advice for the management and conservation of this species.

Author contributions: C.L.D., S.F.D., M.P.M. and P.C. designed the study. C.L.D. and P.C. performed the hydrodynamic model simulations. C.L.D., A.M.K. and M.P.M. analysed the model output and performed statistical analysis. S.F.D. and L.B.F. evaluated the status of reefs, and provided the quality index. C.C. mapped the G.I.S. data. F.L.D.N. provided substantial input on discussion. C.L.D. wrote the first draft of the manuscript and conducted revisions. All authors reviewed the manuscript.

## SUPPORTING INFORMATION

Additional supporting information can be found online in the Supporting Information section at the end of this article.

**How to cite this article:** David, C. L., Marzloff, M. P., Knights, A. M., Cugier, P., Nunes, F. L. D., Cordier, C., Firth, L. B., & Dubois, S. F. (2022). Connectivity modelling informs metapopulation structure and conservation priorities for a reef-building species. *Diversity and Distributions*, *00*, 1–15. https://doi.org/10.1111/ddi.13596